



Design of a CPSS-based reflectarray cell with controllable reflected phase for dual-circularly-polarised reflectarrays

Simon Mener, Raphaël Gillard, Ronan Sauleau, Cécile Cheymol, Patrick Potier

► To cite this version:

Simon Mener, Raphaël Gillard, Ronan Sauleau, Cécile Cheymol, Patrick Potier. Design of a CPSS-based reflectarray cell with controllable reflected phase for dual-circularly-polarised reflectarrays. International Symposium of ANtenna Technology and applied ElectroMagnetics, Jun 2012, Toulouse, France. pp.MENER. hal-00771355

HAL Id: hal-00771355

<https://hal.science/hal-00771355>

Submitted on 8 Jan 2013

HAL is a multi-disciplinary open access archive for the deposit and dissemination of scientific research documents, whether they are published or not. The documents may come from teaching and research institutions in France or abroad, or from public or private research centers.

L'archive ouverte pluridisciplinaire **HAL**, est destinée au dépôt et à la diffusion de documents scientifiques de niveau recherche, publiés ou non, émanant des établissements d'enseignement et de recherche français ou étrangers, des laboratoires publics ou privés.

Design of a CPSS-based reflectarray cell with controllable reflected phase for dual-circularly-polarised reflectarrays

S. Mener¹, R. Gillard¹, R. Sauleau², C. Cheymol³, P. Potier⁴

¹ European University of Brittany, INSA, IETR, UMR CNRS 6164, 35708 Rennes, simon.mener@insa-rennes.fr, raphael.gillard@insa-rennes.fr

² University of Rennes 1, IETR, UMR CNRS 6164, 35042 Rennes, ronan.sauleau@univ-rennes1.fr

³ French space agency CNES, 31401, Toulouse CEDEX 9, France, Cecile.Cheymol@cnes.fr

⁴ DGA Maîtrise de l'information, BP 57419, 35174, Bruz CEDEX, France, patrick.potier@dga.defense.gouv.fr

Full Paper — A first step towards the design of dual-circularly polarised reflectarrays with independent control of both polarisations is proposed in X-band. A reconfigurable unit-cell based on a circularly-polarised selective surface is studied at 8.5 GHz. It provides a 2-bit phase resolution in reflection for the left hand circular polarisation (LHCP) and is nearly transparent in right hand circular polarisation (RHCP). The simulated characteristics are excellent over a 6.4% bandwidth. The proposed unit-cell is fabricated using stacked substrates. A loss budget demonstrates that loss is quite balanced between loss in materials and polarisation conversion. Then, a study of the effect of realistic switches is shown in order to demonstrate that conventional p.i.n. diodes would cause an acceptable loss increase.

Keywords- Circular polarisation selective surface; Unit-cell; Reflectarray.

I. INTRODUCTION

Reconfigurable reflectarrays are very attractive for beam scanning or beam-shaping in space applications. In order to prevent from loss due to polarisation misalignment and increase the data rate transmission, circular polarisation (CP) is usually preferred. Several circularly-polarised unit-cells have been proposed in the literature [1], [2], but they only operate with one single CP wave. Reconfigurable unit-cells with independent control of the reflected phases in both circular polarisations are still required in order to increase the data-rates.

In this paper, we propose to use a unit-cell based on a circular polarisation selective surface (CPSS) in order to provide a dual-circular polarisation operation. Fig. 1 illustrates the operation principle of the proposed two-layer structure. The upper layer is a CPSS reflecting LHCP with a controllable reflection phase, while RHCP is transmitted to the second layer that reflects it with an independent controllable reflection phase shift. This second layer operates in single polarisation and only requires standard CP unit-cells as for instance [3]. This paper deals with the first layer only. The objectives are to achieve a high isolation between the two incident circular polarisations and a 2-bit phase resolution of the reflected LHCP polarisation. Moreover, the

loss budget is studied in order to assess the respective impact of polarisation conversion and dissipation in materials. It is then extended to account for loss in switches controlling the reflected phase, as a first evolution towards an active cell.

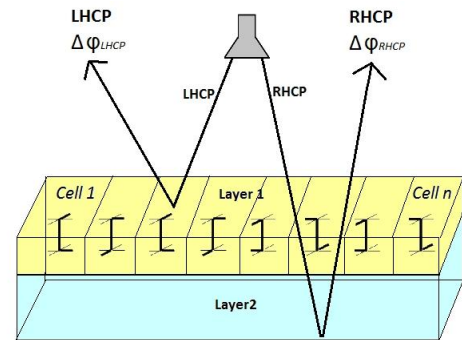


Figure. 1. Schematic representation of a reflectarray with independent control of both incident circular polarisations.

II. DESCRIPTION OF THE UNIT-CELL

The basic configuration of the chosen Left-Handed CPSS (LH-CPSS) cell (Fig. 2) is derived from [4]. It consists of a 1λ -long resonant wire, folded into 3 segments in a crank-like shape. The transverse segments ($3\lambda/8$ long) are connected by a $\lambda/4$ long longitudinal segment; this ensures that the currents induced on the transverse segments (by an impinging wave under normal incidence) are in phase or out of phase, depending of the hand of the incident CP wave.

Fig. 2 represents a typical printed implementation (using the stacked substrate defined in [5]) of the resonant crank. In the following, this configuration is referred to as “state 1”. It is well known that the reflected phase of a CP wave can be tuned by varying the angular rotation of the reflecting element [6]. Consequently, different reflected phase values can be obtained by introducing several cranks in the same unit-cell with an appropriate rotation angle. So, to achieve four different LHCP reflected phases (namely a 2-bit phase resolution), four different sets of horizontal segments are used. Only one of them is enabled at a time by connecting the three segments forming the resonant crank. The optimised proposed unit-cell in state 1 is represented in Fig. 3. The active crank is represented in red, while the three

passive ones are shown in blue. As can be seen, in this figure, small gaps are accommodated along the horizontal segments. As a consequence, in a future active version of the cell, switches could be used to connect or disconnect the different metallic parts forming a resonant crank. In this paper, only frozen states are considered which means ideal short and open circuits replace the switches. The final design does not only rely on a rotation of the crank; the size and shape of the different segments have also been optimised in order to comply with both the technological constraints (available surface allocated to the cell, square grid, etc.) and foreseen objective (four possible phase states with uniform-distribution in the $[0,360^\circ]$ range at 8.5 GHz). Phase states 2 to 4, corresponding respectively to a rotation of the activated crank by $+135^\circ$, -90° and -45° degrees are shown in Fig. 4 to 6. For states 2 and 4, the transverse segments of the resonant crank are meandered to accommodate them in the square unit-cell. The length of the different segments is tuned so that all cranks resonate at the same frequency (8.5 GHz).

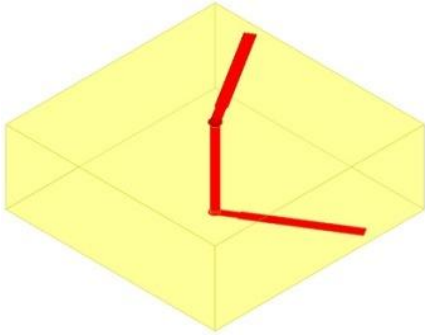


Figure 2. Basic LH-CPSS.

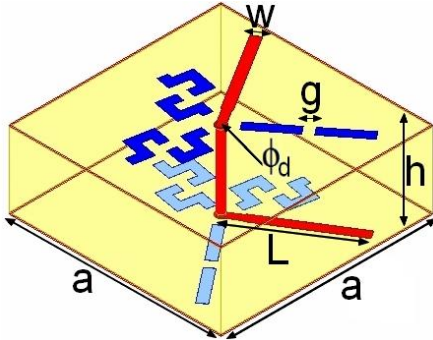


Figure 3. Optimised proposed cell with crank 1 activated: $a=22.88\text{mm}$, $w=1\text{mm}$, $h=8.49\text{mm}$, $g=1\text{mm}$, $L=12.1\text{mm}$, $\phi_d=0.8\text{mm}$.

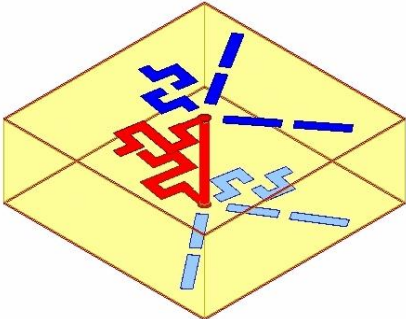


Figure 4. Optimised proposed cell with crank 2 activated

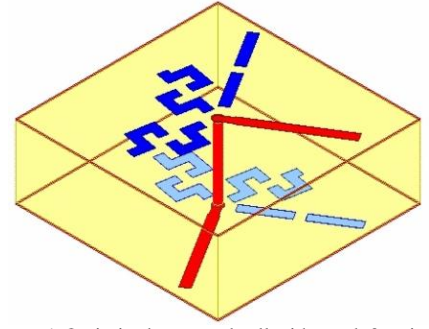


Figure 5. Optimised proposed cell with crank 3 activated

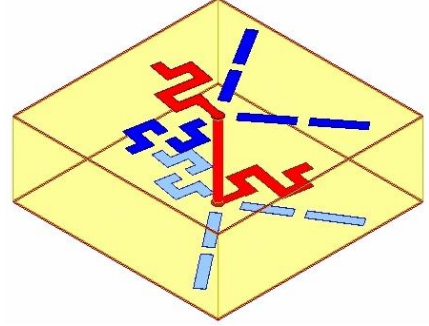


Figure 6. Optimised proposed cell with crank 4 activated

III. PERFORMANCES OF THE UNIT-CELL

The frequency response of the unit-cell has been computed using Ansys HFSS ©. In the simulations, we assume that the cell is suspended in a square metallic waveguide with wave ports at both ends. Figs. 7 and 8 represent the simulated performances for the four possible phase states.

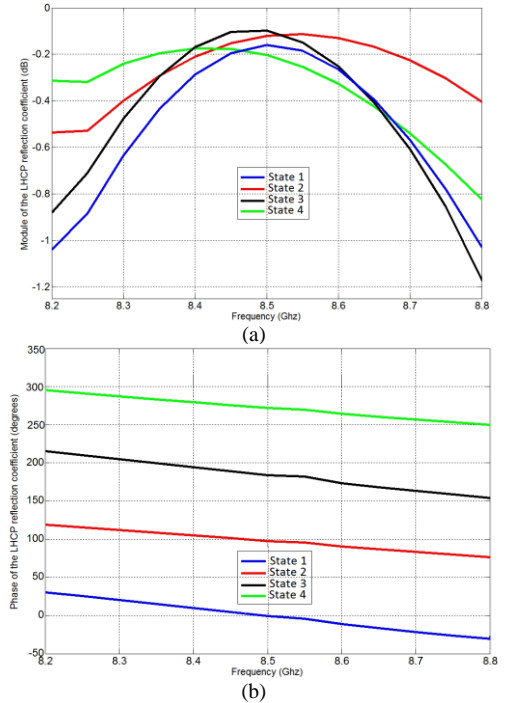


Figure 7. Reflection coefficient for an incident LHCP wave for the four activated crank of the cell. (a) Magnitude. (b) Phase.

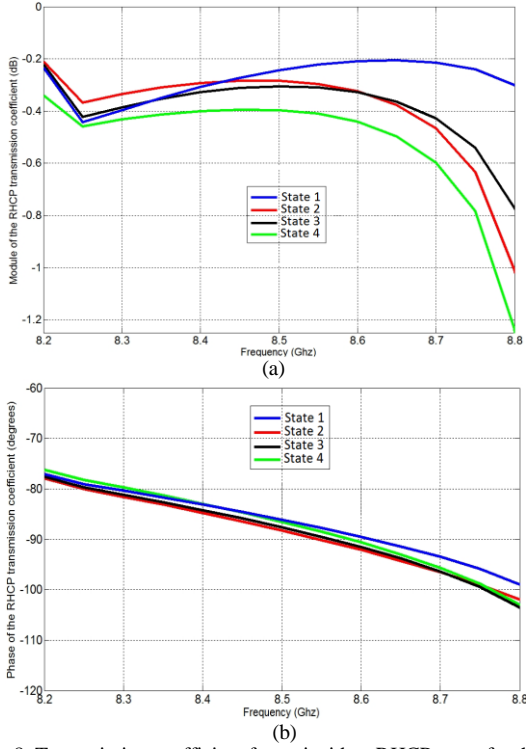


Figure 8. Transmission coefficient for an incident RHCP wave for the four activated crank of the cell. (a) Magnitude. (b) Phase.

Fig. 7a shows that the loss for the reflected LHCP is lower than 1 dB on the [8.2-8.75] GHz range. At the same time, as shown in Fig. 8a, for the four phase-states (in LHCP), the RHCP incident wave is transmitted through the LH-CPSS with insertion loss lower than 1 dB over a 0.55-GHz range (6.4%). The reflection phase responses in LHCP and the transmission phase responses in RHCP between 8.2 and 8.8 GHz are plotted in Figs. 7b and 8b respectively. The reflection coefficient in LHCP shows excellent performances: four 90°-spaced phase configurations are obtained with almost the same frequency dispersion. Moreover, the RHCP wave is transmitted with a nearly constant phase whatever the resonant crank activated.

IV. LOSS BUDGET

A. Loss of the unit-cell in frozen states

In this section, the different possible causes of loss in the cell are investigated. Figs. 9 a and b represent the magnitude of the reflection and transmission coefficients for a LHCP and RHCP incident wave respectively. The cell is in state 1. Two different configurations are considered: in the first one (dashed lines), substrates and metallic segments are lossless; in the second one (continues lines), the characteristics of the actual materials are used: two thin layers (0.127mm-thick) of dielectric substrate (RT/duroid 6002, $\epsilon_r = 2.94$, $\tan\delta = 0.0012$) separated by an 8mm-thick dielectric spacer (foam Rohacell 51HF, $\epsilon_r = 1.06$, $\tan\delta = 0.0015$) and glued by a 0.1mm-thick bonding film. Two conclusions can be drawn: i) loss in the materials is globally small, ii) the effect is however more pronounced for LHCP reflection. This is

due to the resonance of the crank (only obtained for LHCP excitation) which increases the loss in materials. Note that neglecting the loss in the metallic segments (not shown) leaves the results unchanged, which means dielectric loss is prominent. A complete loss budget at the central frequency is given in Table I for the most critical configurations (LHCP incident wave). At the central frequency, the loss in the materials (0.075dB) is comparable to the loss due to polarisation conversion ($\Gamma_{R-L} = 0.035$ dB in reflection and $T_{R-L} = 0.038$ dB in transmission) and the loss due to power leakage of the LHCP wave through the LH-CPSS cell (0.066dB).

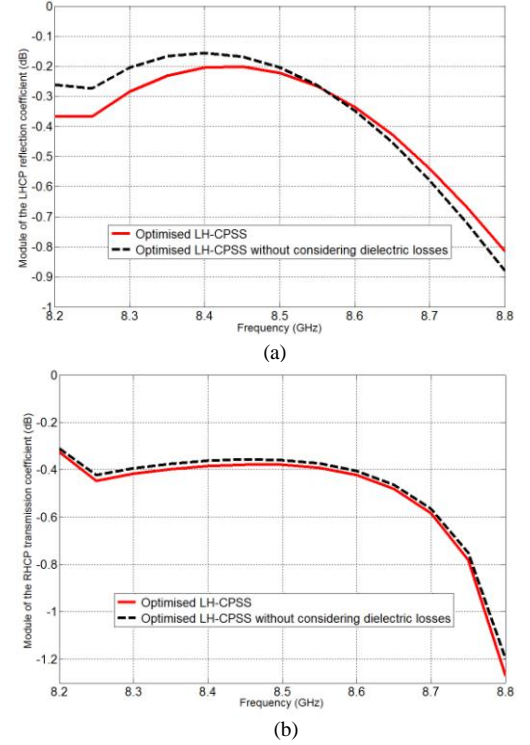


Figure 9. Performance of the optimised LH-CPSS (in State 1) with or without consideration of the dielectric losses. (a) LHCP reflection coefficient. (b) RHCP transmission coefficient

TABLE I
LOSS BUDGET OF THE UNIT-CELL IN FROZEN STATES

	Γ_{L-L}	Γ_{R-L}	T_{L-L}	T_{R-L}	$\sqrt{1 - (\Gamma_{L-L}^2 + \Gamma_{R-L}^2 + T_{L-L}^2 + T_{R-L}^2)}$
Magnitude (linear)	0.975	0.09	0.123	0.094	0.131
Associated loss (dB)		0.035	0.066	0.038	0.075

B. Losses caused by the series resistances of ON-switches

In the previous sections, the studied unit-cell only involved frozen states. As a preliminary step towards the final reconfigurable cell, the additional loss due to the integration of realistic p.i.n. diode switches is now addressed. To do so, ideal short-circuits are replaced by series resistances R_s accounting for the parasitic resistance of the diode in the ON-state. Note that four resistances are

necessary for the activated crank. In this study, we do not account for the effect of OFF-switches. Indeed, these switches will mainly act as a capacitive loading and this reactive effect could be compensated by a re-optimisation of the dimension of the metallic segments. Nevertheless, the impact on loss should be negligible. Fig. 10 shows the top view of the unit-cell in state 1 with the series resistance R_s replacing the ideal short-circuits. Fig. 11 presents the magnitude of reflection and transmission coefficients for different values of the resistance.

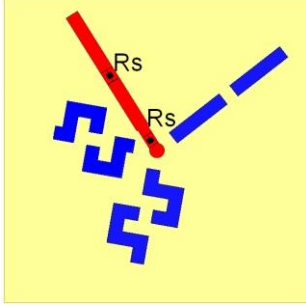


Figure 10. Top view of the optimised unit-cell in State 1 with the series resistance R_s

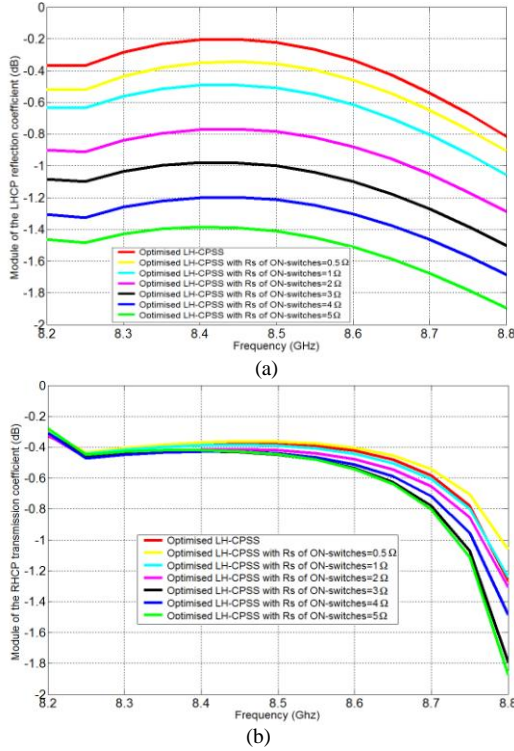


Figure 11. Performances of the optimised LH-CPSS (in State 1) versus the values of the series resistance of the four ON-switches. (a) LHCP reflection coefficient. (b) RHCP transmission coefficient

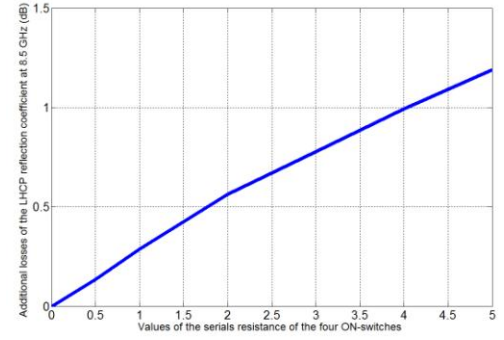


Figure 12. Additional losses of the LHCP reflection coefficient at 8.5 GHz versus to the values of the serial resistance of the four ON-switches.

As previously, the effect is more significant for the reflection of a LHCP incident wave. Fig. 12 plots the additional loss versus the resistance value at 8.5 GHz. For a typical value of 2Ω , it is about 0.6 dB.

V. CONCLUSION

A new design of CPSS unit-cell has been proposed for dual circularly-polarised reflectarray applications. It provides a nearly 2-bit phase resolution in reflection for the left hand circular polarisation (LHCP) and is almost transparent in right hand circular polarisation (RHCP). Furthermore, the insertion loss for the reflected LHCP and transmitted RHCP is lower than 1 dB over the [8.2-8.75] GHz range. A loss budget demonstrates that loss is balanced between loss in materials, polarisation conversion and power leakage through the reflecting structure. A preliminary study of the effect of realistic switches shows that conventional p.i.n. diodes would cause an acceptable 0.6 dB loss increase.

REFERENCES

- [1] J. H. Wang, "Characteristics of a new class of diode-switched integrated antenna phase shifter," *IEEE Trans. Antennas Propag.*, vol. 31, no. 1, pp. 156-159, Jan. 1983.
- [2] E. Martynyuk, J. I. Martinez Lopez, and N. A. Martynyuk, "Reflectarray based on three bit spatial phase shifters: mathematical model and technology of fabrication," *Proceedings of the 3rd European Conference Antennas and Propag.*, Berlin, Germany, 23-27 Mar. 2009.
- [3] E. Girard, R. Moulinet, and R. Gillard, "An FDTD optimization of a circularly polarized reflectarray unit cell," *IEEE Antennas Propag. Soc. Int. Symposium*, San Antonio, TX, vol. 3, pp. 136-139, Jun. 2002.
- [4] J. E. Roy and L. Shafai, "Reciprocal circular-polarization selective surface," *IEEE Antennas Propag. Mag.*, vol. 38, no. 6, pp. 18-33, Dec. 1996.
- [5] S. Mener, R. Gillard, R. Sauleau, C. Cheymol, and P. Potier, "A CPSS-based reflectarray cell with reconfigurable capabilities," *Proceedings of the 6th European Conference Antennas and Propag.*, Prague, Czech Republic, 26-30 Mar. 2012.
- [6] J. Huang, J.A. Encinar, "Reflectarray antennas", Wiley-IEEE Press, ISBN: 978-0-470-08491-5, November 2007